Extralymphatic Tumors Prepare Draining Lymph Nodes to Invasion via a T-Cell Cross-Tolerance Process

Olivier Preynat-Seauve,[1] Emmanuel Contassot,[1] Prisca Schuler,[1] Vincent Piguet,[2] Lars E. French,[1] and Bertrand Huard[1]

[1]Louis Jeantet Skin Cancer Laboratory, Departments of Dermatology and Patho-Immunology, University Medical Center and [2]Department of Dermatology and Venereology, University Hospital of Geneva, Geneva, Switzerland

Abstract

Metastases often develop in lymphoid organs. However, the immunologic mechanism allowing such invasion is not known because these organs are considered to be hostile to tumor cells. Here, we analyzed the interactions between tumor cells and $CD8^+$ T cells in such lymphoid organs. Tumor cells implanted into lymph nodes were able to induce tumor-specific cytotoxic $CD8^+$ T-cell responses, conducting to tumor rejection, in contrast to primary extralymphatic tumors rapidly anergizing T cells in draining lymph nodes (DLN) via a cross-presentation process. This abortive $CD8^+$ T-cell response to extralymphatic tumor is independent of the subcellular localization of antigen in tumor cells and is consistent with a lack of $CD4^+$ T-cell help. Notably, this anergy was potent enough to allow successful DLN implantation of tumor cells. Such distant cross-tolerization of tumor-specific $CD8^+$ T cells may be a determinant permissive event leading to invasion of DLN. In this situation, metastatic tumor cells do not need to down-regulate their immunogenicity to spread. [Cancer Res 2007;67(10):5009–16]

Introduction

Propagation of metastatic tumor cells is responsible for 90% of human cancer deaths (1). The spreading process often starts in tumor-draining lymph nodes (TDLN; ref. 2). However, it is not understood why metastases can develop in lymphoid organs because these organs constitute a hostile environment for tumor cells (3). In addition, although it is widely accepted that tumor nests constitute immunoprivileged sites (4), there is no evidence that such local tumor immunosuppression is involved in metastatic invasion of distant organs. Loss of immunogenicity has been one putative explanation for metastasis in lymphoid organs (5). However, recent gene expression array studies have shown that the molecular signatures of metastatic cells and primary tumor cells from which they originate are very similar in diverse cancers (6, 7). In this respect, loss of immunogenicity is also observed at the level of primary tumor cells (5). These data suggest that loss of immunogenicity may not be an essential step in metastasis. By studying interactions between tumor and host T cells in lymph nodes draining or not a primary tumor, we observed that tumor cells do not need to lose their immunogenicity to invade TDLN organs.

Materials and Methods

Mice, cells, and reagents. All animal procedures and husbandry were carried out in accordance with Swiss federal regulations. Nonobese diabetic severe combined immunodeficient (NOD SCID) and C57BL/6 mice were bred in house. OT-I and OT-II mice were obtained from W. Heath (University of Melbourne, Victoria, Australia). Green fluorescent protein (GFP)–labeled OT-I T cells were generated by crossing OT-I and mice with GFP-transgenic mice (kindly provided by Dr. M. Okabe, Osaka University, Osaka, Japan). For the generation of chimeric mice, donor bone marrow cells from C57Bl/B6 ($H\text{-}2^b$) or DBA-2 ($H\text{-}2^d$) mice were obtained from femurs and tibiae. Twenty hours after total body irradiation (1,000 rad), B6D2F1 ($H\text{-}2^b \times H\text{-}2^d$) mice received 10×10^6 sex-matched bone marrow cells in a lateral tail vein. Seven weeks after transplantation, H-2 phenotypes of grafted recipients were determined by immunostaining of peripheral blood cells with $H\text{-}2^b$– and $H\text{-}2^d$–specific monoclonal antibody (mAb). Reconstitution efficiency was >95% in all chimeras.

The B16F10 melanoma was kindly provided by I. Fidler (University of Texas, Houston, TX). MC38, CMT93, and EL-4 were obtained from the American Type Culture Collection.

$Ovalbumin_{257–264}$ ($OVA_{257–264}$; SIINFEKL), $OVA_{323–339}$ (ISQAVHAAHAEINEAGR), and control $gp33_{33–41}$ from LCMV (KAVYNFATM) peptides were synthesized according to the F-moc strategy at the Lausanne Biochemistry Institute (Lausanne, Switzerland). Purified OVA, complete Freund adjuvant (CFA), lipopolysaccharide, peptidoglycan, poly-IC, and lipoteichoic acid was obtained from Sigma. The ODN 1826 containing CpG sequences were obtained from Coley Pharmaceuticals. Cisplatin and doxorubicin were kindly provided by P.Y. Dietrich (University of Geneva, Geneva, Switzerland). MegaFas-L, MegaTNFα, and MegaCD40-L described elsewhere (8) have been obtained from P. Schneider (University of Lausanne, Epalinges, Switzerland). $H\text{-}2K^b/OVA_{257–264}$ tetramers were prepared according to Kalergis et al. (9). For $CD8^+$ T-cell depletion, 100 μg of the rat anti-mouse CD8 (H35) were injected i.p. at days −8 and −5 before intralymphatic implantation and OT-I T-cell transfer, respectively. Isotype control was the rat IgG Dave II (Apotech). Fluorochrome-conjugated anti-CD4, CD8, CD44, CD69, $H\text{-}2^b$, $H\text{-}2^d$, Fas, and IFN-γ were all from PharMingen.

Engineering of tumor cells expressing secreted, membrane, and cytoplasmic OVA. Full-length OVA cDNA encoding for secreted OVA was kindly provided by Dr. M. Bevan (University of Washington, Seattle, WA) and subcloned into pCDNA3.1(+) (Invitrogen AG). PCDNA3.1(+)/OVA was modified to express cytoplasmic and membrane OVA. Briefly, the cytoplasmic form of OVA was obtained by PCR-created deletion of the first 45 amino acids containing the sequence necessary for OVA secretion (10). To generate the membrane form of OVA, a PCR product containing the transmembrane and cytoplasmic part of hOX40L ($hOX40L_{1–61}$) was generated and cloned upstream of the OVA cytoplasmic form. Tumor cells were transfected with plasmids encoding OVA by electroporation and selected with G418 (Invitrogen). A clone for B16-OVAcyt was first selected for an OVA expression close to endogenous tyrosinase by quantitative reverse transcription-PCR (RT-PCR). The selected B16-OVAcyt cell clone served as standard (OVA expression of 1) for the other OVA-expressing tumors. This B16-OVAcyt cell clone was supertransfected with human Fas cDNA subcloned into a lentiviral vector as described previously (11). The recombinant lentivirus was produced by transient transfection of 293T cells according to standard protocols. Expression of human Fas at the surface of B16-OVA cells was determined by flow cytometry.

Note: Supplementary data for this article are available at Cancer Research Online (http://cancerres.aacrjournals.org/).

O. Preynat-Seauve and E. Contassot contributed equally to this work.

Requests for reprints: Bertrand Huard, Louis-Jeantet Skin Cancer Laboratory, University Medical Center, rue Michel Servet 1, 1211 Geneva 4, Switzerland. Phone: 41-22-379-58-11; Fax: 41-22-379-58-02; E-mail: bertrand.huard@medecine.unige.ch.

doi:10.1158/0008-5472.CAN-06-4494

Quantitative RT-PCR. RNA was extracted from cells using Rneasy Midi Kit (Qiagen AG) and treated with RQ1 DNase (Promega). Quantitative RT-PCR was done as described (12). The primer sequences for OVA were 5′-TAAGGATGAAGACACACAAGCA and 5′-TGATGCCACTCTAAATAAACCA and the probe for OVA was the amplicon obtained with the primer 5′-CAGTGTGTGAAGGAACTG and 5′-TTCCTCCATCTTCATGCG. The primer sequences for tyrosinase were 5′-GGTCGTCACCCTGAAAATCC and 5′-TCGCATAAAACCTGATGGCTA and the probe for tyrosinase was the amplicon obtained with 5′-TGCTTGGGGGCTCTGAAATA and 5′-TCTGCTATCCCTGTGAGTGG.

Tumor implantation. For intralymphatic implantation, 3×10^3 tumor cells were injected into inguinal lymph nodes according to the procedure described (13). Ten days after injection, mice were sacrificed and tumor-injected lymph nodes were harvested and examined under a binocular microscope for tumor take. The relative tumor burden in lymph nodes was assessed by measuring the longest (L) and smallest (l) diameters and the tumor volume was calculated with the following formula $L \times l^2 \times \pi/6$. For s.c. injection, 3×10^3 or 2×10^5 B16 cells were injected (14).

Subcellular fractionation of B16-OVA cells and Western blot analysis. Confluent cultures of B16-OVA cells (10×10^6) were detached with 2 mmol/L EDTA and washed with PBS. Cells were then exposed to cold water supplemented with a cocktail of protease inhibitors (Roche) for hypotonic cell lysis. Cell lysates were centrifuged at $2{,}000 \times g$ for 10 min at 4°C for macrovesicle elimination. Cell lysates were then equilibrated with 100 mmol/L Tris (pH 7.4), 50 mmol/L KCl, 10 mmol/L $MgCl_2$, and 2 mmol/L EGTA before membrane sedimentation at $100{,}000 \times g$ for 1 h at 4°C. Plasma membranes were solubilized in reducing SDS-PAGE buffer, whereas supernatants containing cytoplasm were treated with 100% trichloroacetic acid for protein precipitation. Cytoplasmic proteins were then washed twice with acetone and solubilized with reducing SDS-PAGE buffer. Total protein extracts were boiled for 5 min and subsequently separated by SDS-PAGE and transferred to polyvinylidene difluoride membranes. Membranes were blocked in PBS containing 5% nonfat dry milk and 0.1% Tween 20 overnight at 4°C. Detection was done with a rabbit polyclonal anti-OVA (Sigma) followed by a peroxidase-conjugated anti-rabbit immunoglobulin (Jackson Immunoresearch) and chemiluminescence (Amersham Biosciences).

OT-I and OT-II T-cell activation assays. For *in vitro* coculture experiments, $CD8^+$ T cells from OT-I spleen and lymph nodes were purified by negative selection with a magnetic cell sorter AutoMACS (Miltenyi Biotech). Secretion of IFN-γ by OT-I T cells in *in vitro* coculture with B16 cells was tested in a standard sandwich ELISA (R&D Systems). For *in vivo* experiments, 10×10^6 total spleen and lymph nodes cells from OT-I or OT-II mice were labeled with 1.25 μmol/L 5,6-carboxy-fluorescein-succinimidyl-ester (CFSE, Sigma) and injected i.v. into a lateral tail vein. In some experiments, OT-II T cells primed *in vivo* with a CFA/OVA challenge 14 days before transfer were used. For proliferation, lymph nodes were collected 3 days after transfer, dissociated mechanically, stained with anti-CD8 or anti-CD4 mAb, and CFSE dilution was analyzed by flow cytometry on gated $CD8^+$ or $CD4^+$ T cells. Fluorescence is shown on logarithmic scales. Percentage of divided parental cells and total number of daughter cells were calculated as previously described (15). Briefly, percentage of divided cells was obtained according to the formula $P = [\Sigma\ (n_i/2i) / \Sigma n_i] \times 100$, and the total number of daughter cells according to the formula $N = \Sigma n_i$. In these formulas, n_i is defined as the absolute number of cells for each division rank i and was calculated with the Cell Quest software (BD Biosciences). For *in vivo* cytotoxicity, 8 days after transfer of OT-I cells, animals were i.v. injected with a mixture of differentially CFSE-labeled syngeneic splenocytes used as target cells. Target cells labeled with 0.5 μmol/L CFSE (dull staining) were pulsed with 1 μmol/L of irrelevant peptide (K^b-restricted gp33 peptide from LCMV). Target cells labeled with 5 μmol/L CFSE (bright staining) were pulsed with 1 μmol/L of SIINFEKL peptide. Eighteen hours later, DLNs were harvested and target cells were numerated by flow cytometry. Killing of SIINFEKL-pulsed target cells was calculated. For *ex vivo* IFN-γ production, lymph node cells were incubated at 37°C for 5 h with 1 μmol/L SIINFEKL (or control peptide) and 2 μmol/L monensin. The cell suspension was fixed/permeabilized and stained with anti-CD8 and IFN-γ mAb. For *in vivo* numeration, DLNs were dissociated mechanically. Tumors were dissociated with constant stirring for 90 min at room temperature in HBSS buffer containing 1 mg/mL type IV collagenase (Sigma) and 2 mmol/L EDTA for additional 30 min. Thereafter, CD8 staining was done and OT-I T cells were numerated by flow cytometry directly for OT-I × GFP or after staining with the H2-K^b/SIINFEKL tetramer for wild-type (WT) OT-I.

Detection of endogenous helper T-cell responses. Detection of serum IgG anti-OVA and anti–2,4-dinitrophenol (DNP) was done on plates coated with OVA and DNP-keyhole limpet hemocyanin (1 μg/well), respectively. An anti-mouse IgG conjugated to alkaline phosphatase, both kindly provided by S. Izui (University of Geneva, Geneva, Switzerland), was used. Detection of effector antigen–specific helper T cells was done as previously described (16). Briefly, 200 μg DNP-OVA (4/1) were injected i.p. into mice. Seven days later, mice were bled and the presence of serum anti-DNP IgG was tested by ELISA.

***In situ* assessment of tumor cell death.** Tumors were snap-frozen in Tissue-Tek (Sakura) 18 h after treatments. Sections were immunostained with biotinylated anti–active caspase-3 mAb (PharMingen) and revealed by streptABComplex/horseradish peroxidase (DAKO) and 3-amino-9-ethyl-carbazole substrate (Sigma). Images were visualized under light microscopy with Axiophot 1, captured with an Axiocam color charge coupled device camera, and treated on a Pentium III computer with axioVision software (Carl Zeiss AG). Pictures shown correspond to an original ×40 magnification.

Results

$CD8^+$ T cells reject B16 melanoma cells implanted in lymph nodes. We first observed that lymph nodes represent a hostile environment for tumor cell growth. Indeed, although the B16F10 melanoma cell line (B16 hereafter) grew well s.c., these cells were readily rejected when implanted into lymph nodes (Fig. 1*A*). We first tried to study B16 tumor cell interaction with host T cells with the use of anti-murine gp100 $CD8^+$ T cells from transgenic pMel-1 mice (17). However, these transgenic T cells in a naive state were unable to detect *in vivo* presentation of endogenous gp100 from B16 cells (data not shown). To circumvent this problem, we introduced in B16 cells the model tumor antigen, OVA (cytoplasmic fragment 46–386). OVA mRNA expression in the selected transfected B16 clone was 30% of that of endogenous tyrosinase, an accepted tumor rejection antigen (18), making this B16 cell clone a valuable tool to study the immunogenicity of tumor cells expressing a neo-antigen, such as OVA used here. The tumorigenicity of the selected clone was not different to that of the original B16 cell line in immunodeficient mice (data not shown). When implanted into lymph nodes, B16-OVA was rejected similarly to parental B16 cells (see below). Intralymphatic grafting of B16-OVA cells induced the proliferation of i.v. transferred OT-I T cells, specific for the immunodominant peptide of OVA, SIINFEKL, whereas no OT-I T-cell proliferation was observed in lymph nodes implanted with parental B16 cells or injected with a saline solution (Fig. 1*B*). In this situation, T-cell activation was efficient because it led to the generation of cytotoxic T cells from transferred OT-I T cells in the injected lymph nodes (Fig. 1*C*). SIINFEKL-specific cytotoxic T cells were also induced in animals without transferred OT-I T cells. The involvement of immune cells in the rejection of intralymphatic tumor cells was next investigated. B16 parental cells could grow better in lymph nodes from CD8-depleted mice, indicating a role for $CD8^+$ T cells (Fig. 1*D*). The absence of involvement of innate immune cells was shown by the successful intralymphatic grafting in allogeneic NOD SCID animals (Fig. 1*D*). We also used in this experiment as hosts transgenic OT-I mice whose $CD8^+$ T-cell repertoire was constituted by >90% of T cells specific for the SIINFEKL peptide. In these mice, intralymphatic B16-OVA was still rejected similarly

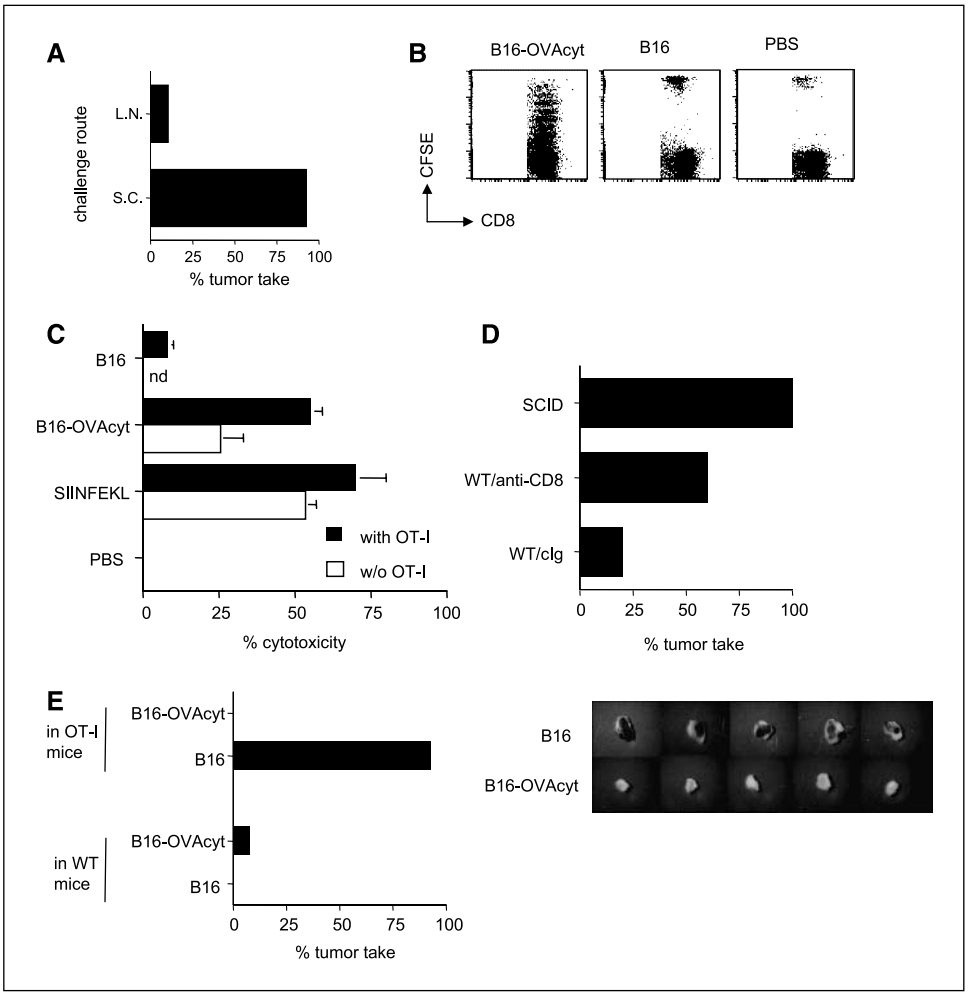

Figure 1. B16 melanoma cells injected into lymph nodes induce tumor-specific CTL leading to rejection. *A,* intralymphatic B16 tumors are rejected. B16 cells (3×10^3) were implanted intralymphatically (*L.N.*) or s.c. Take was assessed in a minimum of 20 mice after nodal and s.c. injection, respectively. *B,* proliferation of OT-I T cells is induced by intralymphatic B16-OVA. CFSE-labeled OT-I T cells were adoptively transferred into WT C57BL/6 mice. One day later, B16 or B16-OVA was injected into inguinal lymph nodes, and OT-I T-cell division was assessed 3 d later. *Dot plots,* CFSE dilution in $CD8^+$ T cells in saline- or tumor-injected lymph nodes. *C,* induction of cytotoxic $CD8^+$ T cells by intralymphatic B16-OVA. B16 tumors and OT-I T cells were injected into mice as in (*B*). Eight days after OT-I T-cell transfer, *in vivo* SIINFEKL-specific cytotoxicity was assessed in DLNs. Mice challenged s.c. with CFA/SIINFEKL served as positive control. SIINFEKL-specific cytotoxicity was also tested in C57BL/6 animals without OT-I T-cell transfer. *Columns,* mean cytotoxicity; *bars,* SD. Representative experiments with groups of five mice. Experiments were done at least thrice. *D,* involvement of $CD8^+$ T cells in the rejection of lymphatic B16 tumor cells. B16 cells were injected into lymph nodes of isotype control- or anti-CD8–depleted C57BL/6 and SCID mice. Tumor growth over a 10-d period for a group of five mice. *E,* B16 or B16-OVA was injected into lymph nodes of OT-I transgenic or WT C57BL/6 mice. Tumor growth over a 10-d period in a minimum of 10 mice per group (*left*). Pictures of lymph nodes from OT-I mice injected with the indicated tumors (*right*).

to WT mice, but take of the parental B16 cells was observed in OT-I mice (Fig. 1*E*), showing the importance of tumor antigen–specific $CD8^+$ T cells in the rejection process. Taken together, these experiments indicate that tumoricidal $CD8^+$ T cells are induced in the presence of tumor cells in lymph nodes, conducting to tumor rejection in this organ.

$CD8^+$ T cells are cross-activated by extralymphatic B16 tumors in TDLN. We next studied interactions of $CD8^+$ T cells when tumor cells were growing extralymphatically. To extend our study to differently localized antigens, we generated two other OVA forms—one secreted (OVAsec) corresponding to full-length OVA and one expressed at the cell membrane (OVAmb). B16 clones expressing OVAsec and OVAmb were next selected by quantitative RT-PCR. Clones expressing OVA at 50% of B16-OVAcyt were obtained. No difference in tumor growth was observed between these three selected B16-OVA clones *in vitro* and *in vivo* after grafting in nude mice (data not shown). As expected, OVA was processed and presented onto MHC class I molecules in these clones because it induced IFN-γ secretion by OT-I T cells upon *in vitro* coculture (Fig. 2*A*). To ensure that each form of OVA was expressed in specific cell compartments, biochemical detection of OVA was done after subcellular fractionation. OVA was found in the cytoplasm of B16-OVAcyt, the plasmic membrane of B16-OVAmb, and the supernatants of B16-OVAsec culture, respectively (Fig. 2*B*). There was no detection of these forms in other cellular compartments. We analyzed the activation status of OVA-specific $CD8^+$ T cells in TDLNs of s.c. B16-OVA. B16-OVA, when growing s.c., was detected by $CD8^+$ T cells in TDLN (axillary and inguinal), because transferred OT-I T cells proliferated in B16-OVA–bearing mice (Fig. 2*C*). Parental cells ($10.5 \pm 1.2\%$) reaching a TDLN started to divide upon OVA cross-presentation from B16-OVAcyt. A significant difference was observed for the membrane and secreted forms giving lower values, $6.2 \pm 0.5\%$ and $5.8 \pm 0.8\%$ divided parental cells, respectively ($P < 0.05$). Noteworthy, these values were in the range of that obtained with CFA/SIINFEKL challenge ($13 \pm 1\%$; Fig. 2*D*, *left*). The total number of daughter cells obtained with B16-OVAcyt was $9 \pm 1 \times 10^2$ daughter cells (Fig. 2*D*, *right*). We evaluated the input of parental OT-I T cells to average 9×10^2 cells per skin DLNs by SIINFEKL/K^b tetramer staining (data not shown), indicating that the OT-I T-cell population doubled in 3 days in TDLN. In contrast to the percentage of divided cells, the values for OVA associated with B16 cells were much lower than that obtained with peptide in adjuvant ($8 \pm 2.5 \times 10^3$; $P < 0.05$). Taken together, these observations indicate that the recruitment of individual T cells to enter the proliferating pool was quite high in TDLN upon OVA cross-presentation, in the range of a peptide in adjuvant challenge; however, the generation of daughter cell was less potent. During this process, there were no major differences between the three different forms of OVA. In subsequent experiments, the cytoplasmic and secreted forms of OVA representing the less and

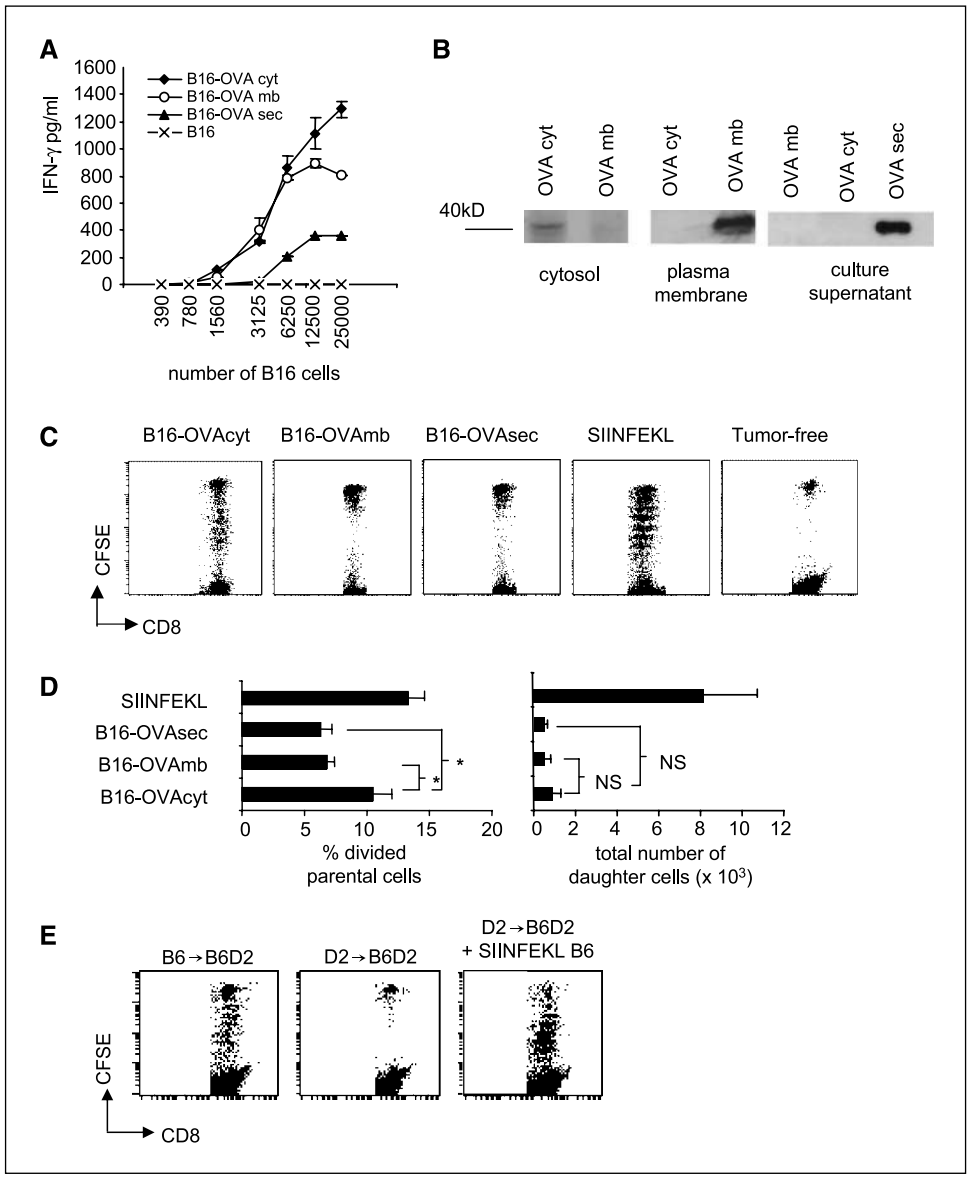

Figure 2. Antigens associated to s.c. B16 tumors are cross-presented to $CD8^+$ T cells in TDLN independently of their subcellular localization. *A,* OVAcyt, OVAsec, and OVAmb are directly presented to OT-I T cells by B16-OVA cells. Irradiated B16 cells were mixed with purified 5×10^5 OT-I T cells. IFN-γ production for a 3-d culture. One representative of three experiments. *B,* subcellular fractionation was done for B16-OVA cell clones and analyzed by Western blot for OVA expression. *C,* OVAcyt, OVAsec, and OVAmb activate similarly OT-I T cells in TDLN. CFSE-labeled OT-I T cells were adoptively transferred into the indicated mice and OT-I T-cell proliferation was analyzed by flow cytometry. *D, left, columns,* mean percentage of parental OT-I T cells that started to divide; *bars,* SD. *Right, columns,* total number of daughter cells generated; *bars,* SD. Analysis was done on groups of five mice. *, $P < 0.05$, statistical difference according to the Student's *t* test. *E,* B16-asociated OVA is cross-presented to OT-I T cells in TDLN. A similar experiment as in (*A*) with B16-OVAcyt was done in B6 ($H\text{-}2^b$) or D2 ($H\text{-}2^d$) reconstituted B6D2F1 mice (*bottom*). B6 splenocytes pulsed with SIINFEKL (1 μg/mL) injected i.v. before OT-I T-cell transfer were used as positive control in $H\text{-}2^d$ reconstituted mice.

most accessible antigens to host immunity, respectively, were preferentially used.

The B16-OVA tumor cells used in this study, as well as the parental cell line, were not metastatic when implanted s.c. Consistent with previous observations (19), we never observed pigmented B16 cells in >100 TDLNs observed, and no B16-OVA cells could be recovered from >20 cultures of TDLN (data not shown). To definitely exclude a direct presentation of tumor antigens by tumor cells, experiments were done in chimeric mice reconstituted with $H\text{-}2^b$ (presenting SIINFEKL) or $H\text{-}2^d$ (not presenting SIINFEKL) bone marrow. OT-I T cells did not proliferate in B6D2F1 ($H\text{-}2^{bxd}$) mice reconstituted with $H\text{-}2^d$ (Fig. 2*E*). In this allogeneic background, transferred OT-I T cells were still reactive to SIINFEKL-pulsed target cells, excluding a putative hybrid resistance mechanism (20) that could suppress OT-I T-cell activation and thus demonstrating a cross-presentation of B16-associated antigens by host bone marrow–derived cells.

Cross-presentation of antigens from B16 extralymphatic tumors does not induce $CD4^+$ helper T cells. We next assessed whether OVA cross-presentation in TDLN was associated with $CD4^+$ T-cell activation. We first looked in sera of tumor-bearing mice for IgG-switched antibodies specific for OVA. Sera from 34 B16-OVAcyt– and 6 B16-OVAsec–bearing mice were tested. A barely detectable reactivity at the lowest serum dilution (1/10) was detected in B16-OVA–bearing mice compared with a challenge of OVA in CFA (Fig. 3*A*). In mice bearing palpable s.c. B16-OVAcyt, the presence of OVA-specific effector helper T cells was tested by a boost with a T cell–dependent antigen (DNP) covalently linked to OVA. Seven days later, the presence of serum IgG against DNP was evaluated. Figure 3*B* shows that IgG against DNP could not be raised in B16-OVA bearing mice, whereas they were generated in mice initially primed with the $OVA_{326-339}$ peptide in CFA. Altogether, this indicates that tumor-associated OVA cross-presentation in TDLN is not associated with induction of effector helper $CD4^+$ T cells.

To dissect the defect in $CD4^+$ T-cell responses against OVA associated to B16, OVA-specific TCR-transgenic OT-II T cells were adoptively transferred in tumor-bearing animals. No cell division

was observed in TDLN, irrespective of the antigen subcellular localization, whereas it was observed in lymph node draining when challenged with soluble OVA in CFA (Fig. 3*C*, *top*). The absence of OT-II T-cell activation was also observed with other s.c. growing tumors transfected with these different forms of OVA, such as the colon carcinomas CMT93 and MC38 and the T-cell lymphoma EL-4, whereas OT-I T cells always detected OVA presentation in TDLN of these tumors (Supplementary Table S1). The absence of OT-II T-cell activation was also observed with the lack of CD69 induction, one of the earliest T-cell activation markers (Fig. 3*C*, *bottom*). A similar absence of proliferation and CD69 induction was also observed when *in vivo* primed OT-II T cells were transferred (data not shown). In addition, OT-II T cells transferred for 8 days in B16-OVA mice were as able as cells from tumor-free mice to proliferate to a CFA/OVA challenge given proximal to the tumor site (data not shown), providing further evidence for a nontolerized naive state. We also tried to induce OT-II T-cell activation in TDLN by intratumoral manipulations (Supplementary Table S2). We first increased the release of OVA by inducing tumor cell death. Neither nonselective cell death induction with chemotherapeutic drugs in B16-OVA nor selective tumor cell death by injecting human Fas-L into B16-OVA tumors transfected with human Fas induced OT-II T-cell proliferation despite the fact that many tumor cells expressed the active form of caspase-3, and were therefore dying, 18 h after treatment (Supplementary Fig. S1). The same was true when dendritic cell maturating agents were injected intratumorally (Supplementary Table S2). Neither a cocktail of TLR agonists, CD40-L, and tumor necrosis factor α nor CFA could induce OT-II T-cell proliferation in TDLN. OT-II T-cell activation was only observed with soluble OVA was injected into B16 tumors. Hence, presentation of OVA associated to B16 onto host MHC class II molecules in TDLN was an inefficient process; thus, OT-II T cells ignored the antigen in TDLN.

Cross-presentation of antigens from B16 extralymphatic tumors tolerizes CD8$^+$ T cells in TDLN. Cross-activation resulted in the accumulation of antigen-experienced CD44^{high} tetramer$^+$ OT-I T cells in TDLN 8 days after transfer (Fig. 4*A*, *top*). However, nearly no OT-I T cells could be detected at the tumor site by tetramer staining or with the use of GFP$^+$OT-I$^+$ T cells so as to exclude possible TCR down-regulation at the tumor site (Fig. 4*A*, *bottom*). This indicates that despite proliferation, OT-I T-cell cross-activation was not complete. The abortive OT-I T-cell response was confirmed by an *in vivo* cytotoxicity assay because no significant SIINFEKL-specific cytotoxicity was detected in TDLN from B16-OVAcyt and B16-OVAsec 8 days after transfer (Fig. 4*B*). *In vivo* restimulation of cross-activated OT-I T cells accumulating in TDLN was next tested. The percentage of tetramer$^+$ cells among total CD8$^+$ T cells increased in tumor-free mice by 4-fold after a CFA/SIINFEKL challenge proximal to the tumor site, but not in TDLN from B16-OVAcyt (Fig. 4*C*). IFN-γ production was also tested in an *ex vivo* restimulation assay with the SIINFEKL peptide. No intracellular IFN-γ production was detected in OT-I T cells from

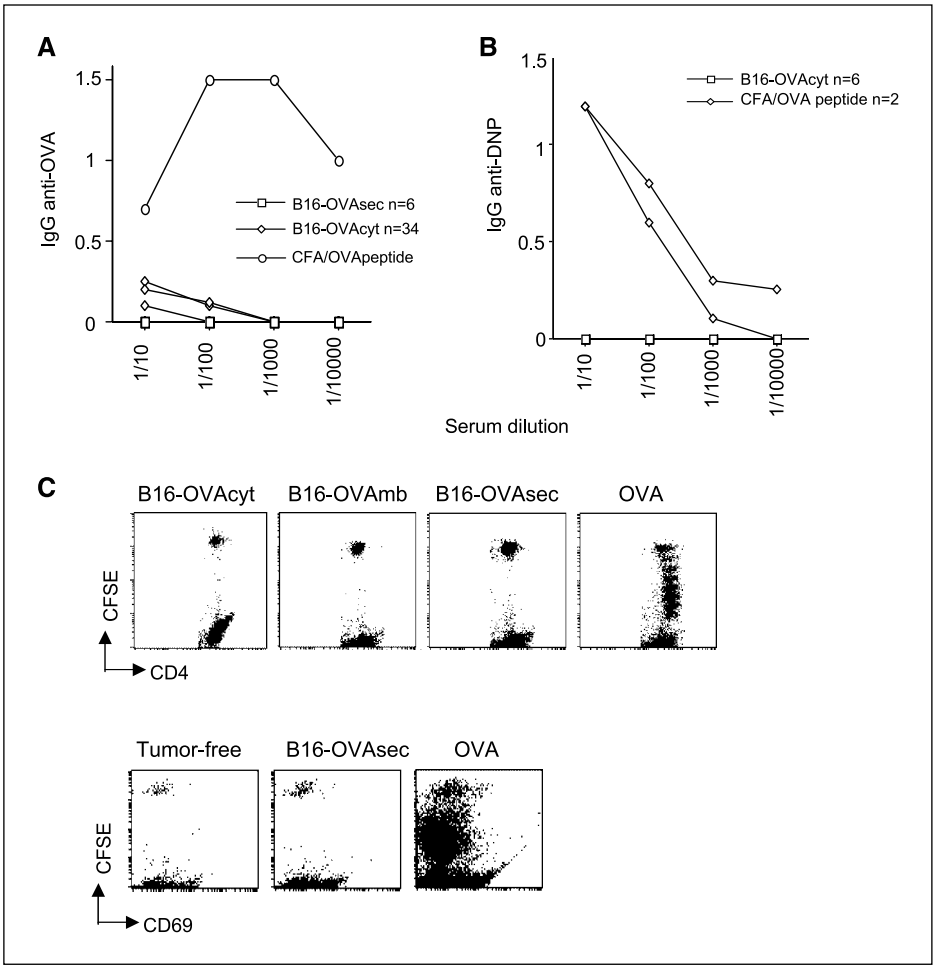

Figure 3. OVA associated to B16 does not activate CD4$^+$ T cells in TDLN. *A,* absence of anti-OVA IgG in B16-OVA–bearing mice. Sera were collected when tumor surfaces were between 0.5 and 1 cm^2. The IgG anti-OVA in mice challenged with CFA/OVA is representative of six animals and was tested 7 d after challenge. *B,* absence of OVA-specific helper CD4$^+$ T cells in B16-OVA–bearing mice. Mice primed with $OVA_{326–339}$ in CFA (day −7) or bearing a palpable B16-OVAcyt tumor were boosted with OVA conjugated to DNP. Anti-DNP IgG was tested 7 d later by ELISA. Serum IgG reactivity against DNP for individual mice. *C,* absence of CD4$^+$ T-cell activation in TDLN. CFSE-labeled OT-II T cells were adoptively transferred into the indicated mice. Cell proliferation was analyzed as in Fig. 2*C* in mice bearing B16-OVAcyt, B16-OVAsec, and B16-OVAmb (*top*). CD69 induction on OT-II T cells was also monitored in TDLN from B16-OVAsec (*bottom*).

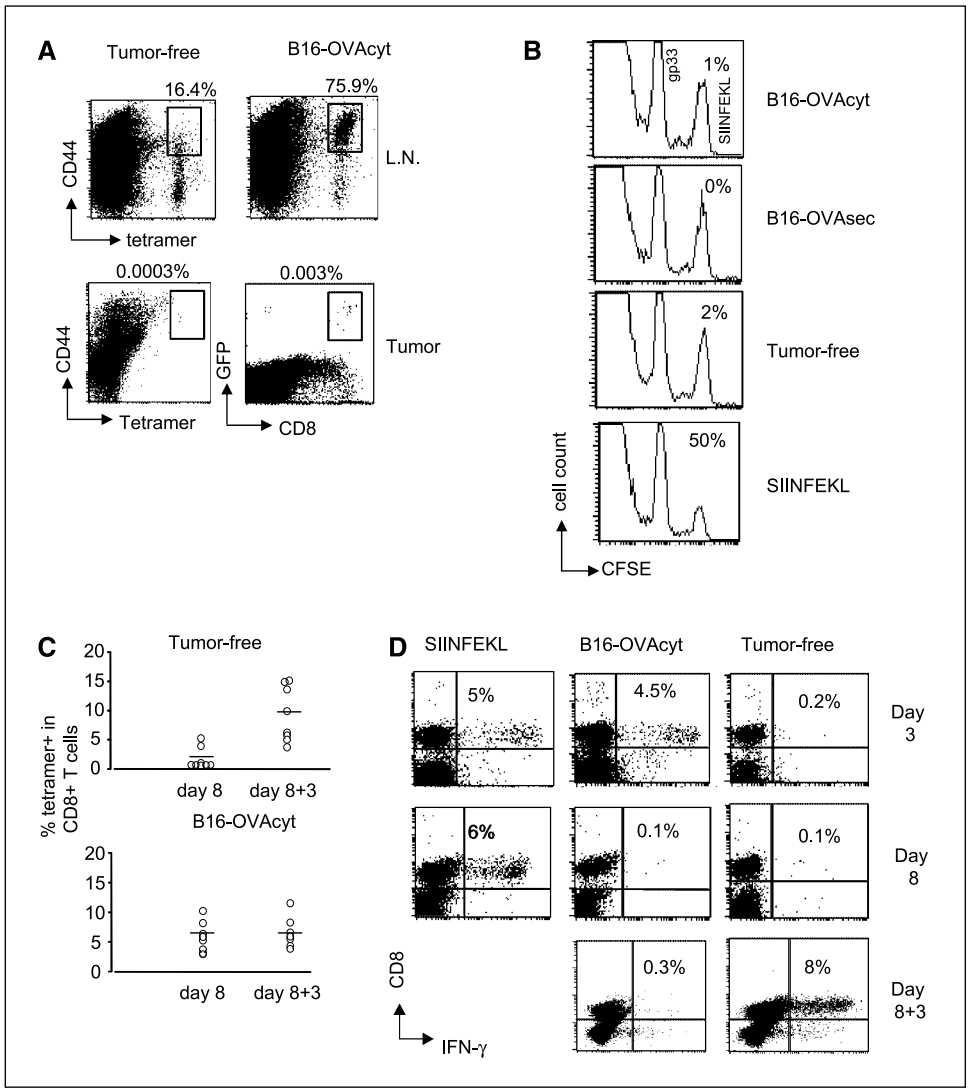

Figure 4. Rapid cross-tolerization of CD8$^+$ T cells in TDLN. *A,* cross-presentation of B16-associated antigens induces the accumulation of antigen-experienced CD8$^+$ T cells in TDLN. Eight days after transfer, OT-I T cells recovered from TDLN and control lymph nodes from tumor-free animals were assessed for CD44 expression by flow cytometry. *Top dot plots,* CD44 expression on tetramer$^+$ cells. The percentage of CD44^{high} cells among tetramer$^+$ cells is indicated. Migration of OT-I T cells to the tumor site was studied 8 d after transfer with the use of tetramer staining or GFP$^+$ OT-I T cells. *Bottom dot plots,* the percentage of CD44$^+$tet$^+$ and CD8$^+$GFP$^+$ cells at the tumor site. B16-OVAcyt was used in this experiment. *B,* no induction of cytotoxic CD8$^+$ T cells upon B16 antigen cross-presentation. A SIINFEKL-specific cytotoxicity assay was done 8 d after transfer of OT-I T cells in the indicated mice. Histogram plots showing the different fluorescent cell populations recovered 18 h later from TDLN. Values represent specific killing of SIINFEKL-pulsed target cells (mean ± SD). *C,* OT-I T cells are unable to reproliferate to a peptide challenge. OT-I T cells were numerated with K^b/SIINFEKL tetramer staining 8 d after transfer in a first group of mice. A s.c. CFA/SIINFEKL challenge proximal to the tumor site was done 8 d after OT-I T-cell transfer in a second group of mice. OT-I T cells were numerated 3 d after this challenge (*day 8+3*). B16-OVAcyt was used in this experiment. *D,* cross-activated OT-I T cells are rapidly unable to produce IFN-γ. Three and eight days after OT-I T cell transfer, *ex vivo* SIINFEKL restimulation was done and intracellular IFN-γ was assessed in OT-I T cells. In some experiments, a CFA/SIINFEKL challenge was done as in (*C*), and IFN-γ production was tested *ex vivo* upon peptide restimulation 3 d after this challenge. *Dot plots,* CD8$^+$ T cells producing IFN-γ in indicated DLN. Values represent percentages of IFN-γ$^+$ CD8$^+$ T cells. B16-OVAcyt was used in this experiment. Similar results were observed in mice bearing B16-OVAsec.

B16-OVAcyt TDLN 8 days after transfer, whereas it was detected earlier, 3 days after transfer (Fig. 4*D*). In this short-term restimulation experiment, naive T cells from tumor-free mice also did not produce IFN-γ. We therefore tested IFN-γ production after an *in vivo* CFA/SIINFEKL challenge on the same flank as the tumor site to discriminate between naive and unresponsive T cells. Again, no IFN-γ production was observed in OT-I T cells from B16-OVAcyt TDLN, whereas it was observed in tumor-free mice. This experiment shows the inability of cross-activated OT-I T cells to reproduce IFN-γ. Such inability to reproduce IFN-γ was also observed with B16-OVAsec (data not shown). Taken together, these experiments indicate that cross-activated CD8$^+$ T cells transiently differentiated into effector cells able to produce IFN-γ. However, they did not fully differentiate into cytotoxic cells and were rapidly tolerized.

CD8$^+$ T-cell cross-tolerization by s.c. tumors favors intralymphatic tumor development. The cross-tolerance described above by an established s.c. tumor may protect immunogenic tumor cells from rejection in TDLN. To test this hypothesis, we next did intralymphatic tumor cell implantation in the presence of an established s.c. tumor. In situations wherein cross-tolerization by tumor antigens was possible, intralymphatic growth was dramatically changed. Indeed, a s.c. B16 tumor enabled B16 cells to escape rejection in TDLN from WT mice (Fig. 5*A*). This was also the case when a neo-antigen, such as OVA, was expressed in B16, because s.c. B16-OVAcyt prevented intralymphatic rejection of B16-OVAcyt, and s.c. B16 also protected intralymphatic B16-OVAcyt in WT. However, s.c. B16 did not protect intralymphatic B16-OVAcyt in OT-I host mice. These latter mice contained only OVA-specific CD8$^+$ T cells. Hence, CD8$^+$ T cell cross-tolerization by B16-derived antigens is not possible in this situation, indicating that cross-tolerization was necessary to observe the protection in WT mice. In addition, there was no significant enhancement of intralymphatic B16 growth by s.c. B16 in OT-I mice (Fig. 5*B*). This latter experiment excludes mechanisms independent from cross-tolerization as main protective/sustaining factors in our experimental setting. Together, these experiments show that at-distance cross-tolerization of CD8$^+$ T cells by a s.c. tumor protects tumor cells from immune destruction in TDLN.

Discussion

We showed here with the B16 melanoma cell line that lymph nodes are hostile organs for tumor cell development. In our model,

B16 cells were rejected when grafted into lymph nodes, whereas they outgrew their host when implanted s.c. Take of B16 graft in lymph nodes was strongly ameliorated by depletion of $CD8^+$ T cells and was 100% successful in SCID animals, showing that $CD8^+$ T cells were involved in the rejection process. This is consistent with the induction of cytotoxic $CD8^+$ T cells directed against tumor-associated antigens we observed upon lymphatic implantation of tumor cells.

Induction of antitumor cytotoxic T cells in mice-bearing lymph node tumors contrasted with the lack of effective immunity when tumors developed s.c. In this situation of extralymphatic development, tumor outgrowth was not due to host ignorance because cross-presentation of tumor antigens to $CD8^+$ T cells was observed in TDLN. The resulting T-cell cross-activation was abortive, consistent with previous report in other mouse tumor models showing tolerance (21) or limited T-cell activation detectable in TDLN without effect on tumor growth (22). Despite a relatively high number of cross-activated $CD8^+$ T cells entering cell division, the total expansion was relatively low. In addition, the cells did not migrate from the TDLN and did not differentiate into cytotoxic effector T cells. In fact, cross-presentation resulted in induction of tolerance. In the B16 model used here, tolerance was achieved through T-cell anergization. In this process, $CD8^+$ T cells transiently entered an IFN-γ–producing effector state (3 days after transfer) before progressing toward an unresponsive state achieved 8 days after transfer. This process is similar to the transient effector functions described for $CD4^+$ T cells in another tolerance system (23). Anergic $CD8^+$ T cells seemed to persist in tumor-bearing hosts, at least up to animal death, sacrificed in the present study when tumor size reached 1 cm^2. The induced anergy was strong enough to resist a CFA/peptide challenge and was also complete because it affected proliferative and effector functions. In this respect, it is different from the split anergy previously reported affecting either proliferation (24) or cytokine production (25). Notably, the anergy induction was independent of the subcellular localization of the tumor antigen. Indeed, we observed $CD8^+$ T-cell anergy for a cell-sequestered antigen (OVAcyt) as well as for a secreted antigen (OVAsec). This detection by host T cells of an antigen irrespective to its localization in tumor cells confirms a previous report also made with OVA expressed in an immunogenic tumor cell model (26). This indicates that host antigen-presenting cells are fed with tumor-associated antigens and present them to $CD8^+$ T cells no matter where the antigen is expressed. Hence, $CD8^+$ T-cell anergy is likely to occur for a wide range of antigens expressed in poorly immunogenic tumors.

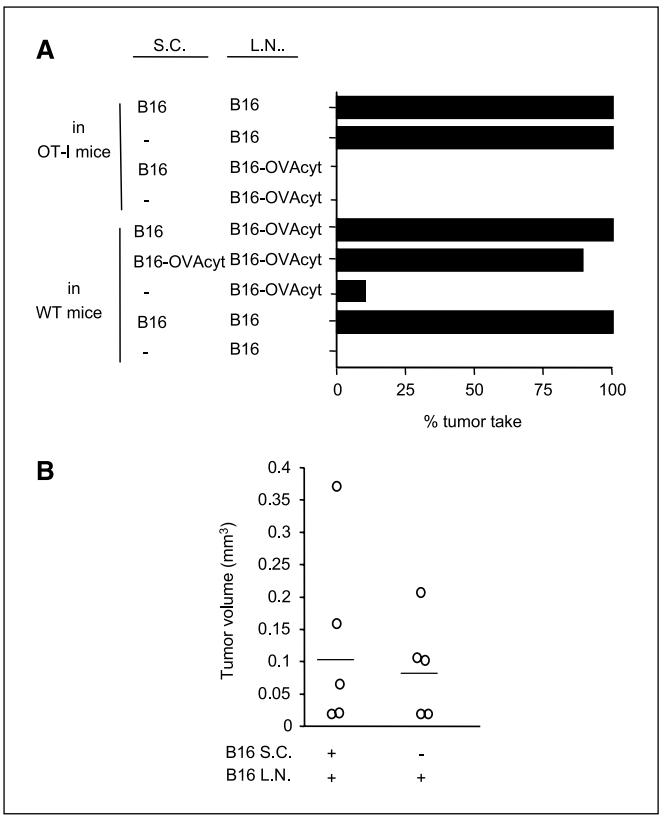

Figure 5. S.c. B16 melanoma favors development of metastases in DLNs in an antigen-specific manner. *A,* induction of B16 growth in lymph nodes by s.c. established B16 tumor cells. B16 or B16-OVA tumor cells (5×10^5) were implanted s.c. into C57BL/6 or OT-I mice. When s.c. tumors were palpable, 3×10^3 B16 or B16-OVA were implanted into TDLN. Tumor take is shown as in Fig. 1*A*. *B,* B16 tumor burden in lymph nodes was compared in tumor-free and in s.c. B16-bearing OT-I mice. Representative experiments with groups of five mice. Experiments were done at least twice.

Antigens associated to B16 are cross-presented by host antigen-presenting cell onto MHC class I to $CD8^+$ T cells in the apparent absence of concomitant presentation onto MHC class II. We saw this dichotomy in the study with a tumor antigen expressed at a physiologic level (30% of the tumor rejection antigen tyrosinase), as well as when this antigen is secreted by the tumor cells, when release of the antigen was increased by induction of tumor cell death or when dendritic cell maturation and trafficking to TDLN were experimentally boosted. This highlighted a profound defect for the cross-presenting dendritic cells to present antigens onto their MHC class II molecules. In this context, it is interesting to note that lymphoid dendritic cells, identified by different groups as the dendritic cell subset responsible for antigen cross-presentation (27, 28), have been recently shown to be poorly efficient to present antigen on their class II molecules (29). Hence, lymphoid dendritic cells may well be the dendritic cell subset cross-presenting B16 antigens in TDLN. The absence of $CD4^+$ T-cell activation in this process is consistent with the abortive $CD8^+$ T-cell response, knowing the strong requirement in $CD4^+$ T-cell help for efficient priming of $CD8^+$ T cells upon antigen cross-presentation (30).

The anergy induced by the primary tumor via cross-presentation of tumor antigen in TDLN is required to facilitate lymphatic invasion of tumor cells. In its absence, when the antigens expressed by primary tumor cells could not be recognized by host $CD8^+$ T cells, there was no development of tumor cells in lymph nodes. This shows that the local immunosuppression observed in the tumor nest is not acting at distance in TDLN and that antigen specificity is the dominant pathway in the protection induced by the primary tumor. In consequence, loss of immunogenicity is not absolutely necessary for metastasis. Sensitivity of metastatic cells developing in lymph nodes to T cell–based immunotherapy was clinically shown with the observed regression of metastatic lesions in melanoma patients responding to the immunotherapy (31). However, it was not known from these data whether the metastatic tumor cells were sensitive to $CD8^+$ T-cell direct killing. Here, we show that metastatic tumor cells invading lymphoid organs may retain their ability to activate T cells and may therefore still be sensitive to $CD8^+$ T-cell cytotoxicity. This observation has important clinical

significance. It strongly suggests that immunotherapy based on the adoptive transfer of tumor-specific T cells is an attractive treatment for residual metastatic diseases.

Acknowledgments

Received 12/6/2006; revised 2/19/2007; accepted 3/8/2007.

Grant support: Association International for Cancer Research, Ligue Suisse contre le Cancer, and Louis-Jeantet Foundation.

The costs of publication of this article were defrayed in part by the payment of page charges. This article must therefore be hereby marked *advertisement* in accordance with 18 U.S.C. Section 1734 solely to indicate this fact.

We thank Shozo Izui and Beat Imhof for critical reading of the manuscript, and Kerstin Grosdemange and Carine Bosshard for their valuable technical assistance.

References

1. Sporn MB. The war on cancer. Lancet 1996;347:1377–81.

2. Santin AD. Lymph node metastases: the importance of the microenvironment. Cancer 2000;88:175–9.

3. Kundig TM, Bachmann MF, DiPaolo C, et al. Fibroblasts as efficient antigen-presenting cells in lymphoid organs. Science 1995;268:1343–7.

4. Zou W. Immunosuppressive networks in the tumour environment and their therapeutic relevance. Nat Rev Cancer 2005;5:263–74.

5. Bubenik J. Tumour MHC class I downregulation and immunotherapy (review). Oncol Rep 2003;10:2005–8.

6. Ramaswamy S, Ross KN, Lander ES, et al. A molecular signature of metastasis in primary solid tumors. Nat Genet 2003;33:49–54.

7. Haqq C, Nosrati M, Sudilovsky D, et al. The gene expression signatures of melanoma progression. Proc Natl Acad Sci U S A 2005;102:6092–7.

8. Holler N, Tardivel A, Kovacsovics-Bankowski M, et al. Two adjacent trimeric Fas ligands are required for Fas signaling and formation of a death-inducing signaling complex. Mol Cell Biol 2003;23:1428–40.

9. Kalergis AM, Goyarts EC, Palmieri E, et al. A simplified procedure for the preparation of MHC/peptide tetramers: chemical biotinylation of an unpaired cysteine engineered at the C-terminus of MHC-I. J Immunol Methods 2000;234:61–70.

10. Meek RL, Walsh KA, Palmiter RD. The signal sequence of ovalbumin is located near the NH_2 terminus. J Biol Chem 1982;257:12245–51.

11. Arrighi JF, Pion M, Wiznerowicz M, et al. Lentivirus-mediated RNA interference of DC-SIGN expression inhibits human immunodeficiency virus transmission from dendritic cells to T cells. J Virol 2004;78:10848–55.

12. Huard B, Arlettaz L, Ambrose C, et al. BAFF production by antigen-presenting cells provides T cell co-stimulation. Int Immunol 2004;16:467–75.

13. Maloy KJ, Erdmann I, Basch V, et al. Intralymphatic immunization enhances DNA vaccination. Proc Natl Acad Sci U S A 2001;98:3299–303.

14. Preynat-Seauve O, Schuler P, Contassot E, et al. Tumor-infiltrating dendritic cells are potent antigen-presenting cells able to activate T cells and mediate tumor rejection. J Immunol 2006;176:61–7.

15. Wells AD, Gudmundsdottir H, Turka LA. Following the fate of individual T cells throughout activation and clonal expansion. Signals from T cell receptor and CD28 differentially regulate the induction and duration of a proliferative response. J Clin Invest 1997;100:3173–83.

16. Ochsenbein AF, Klenerman P, Karrer U, et al. Immune surveillance against a solid tumor fails because of immunological ignorance. Proc Natl Acad Sci U S A 1999;96:2233–8.

17. Overwijk WW, Theoret MR, Finkelstein SE, et al. Tumor regression and autoimmunity after reversal of a functionally tolerant state of self-reactive $CD8^+$ T cells. J Exp Med 2003;198:569–80.

18. Brichard V, Van Pel A, Wolfel T, et al. The tyrosinase gene codes for an antigen recognized by autologous cytolytic T lymphocytes on HLA-A2 melanomas. J Exp Med 1993;178:489–95.

19. Ochsenbein AF, Sierro S, Odermatt B, et al. Roles of tumour localization, second signals and cross priming in cytotoxic T-cell induction. Nature 2001;411:1058–64.

20. Kumar V, George T, Yu YY, et al. Role of murine NK cells and their receptors in hybrid resistance. Curr Opin Immunol 1997;9:52–6.

21. van Mierlo GJ, den Boer AT, Medema JP, et al. CD40 stimulation leads to effective therapy of CD40(−) tumors through induction of strong systemic cytotoxic T lymphocyte immunity. Proc Natl Acad Sci U S A 2002;99:5561–6.

22. Nguyen LT, Elford AR, Murakami K, et al. Tumor growth enhances cross-presentation leading to limited T cell activation without tolerance. J Exp Med 2002;195:423–35.

23. Huang CT, Huso DL, Lu Z, et al. $CD4^+$ T cells pass through an effector phase during the process of *in vivo* tolerance induction. J Immunol 2003;170:3945–53.

24. Ohlen C, Kalos M, Cheng LE, et al. CD8(+) T cell tolerance to a tumor-associated antigen is maintained at the level of expansion rather than effector function. J Exp Med 2002;195:1407–18.

25. Vezys V, Olson S, Lefrancois L. Expression of intestine-specific antigen reveals novel pathways of CD8 T cell tolerance induction. Immunity 2000;12:505–14.

26. Shen L, Rock KL. Cellular protein is the source of cross-priming antigen *in vivo*. Proc Natl Acad Sci U S A 2004;101:3035–40.

27. den Haan JM, Lehar SM, Bevan MJ. CD8(+) but not CD8(−) dendritic cells cross-prime cytotoxic T cells *in vivo*. J Exp Med 2000;192:1685–96.

28. Belz GT, Behrens GM, Smith CM, et al. The CD8α(+) dendritic cell is responsible for inducing peripheral self-tolerance to tissue-associated antigens. J Exp Med 2002;196:1099–104.

29. Dudziak D, Kamphorst AO, Heidkamp GF, et al. Differential antigen processing by dendritic cell subsets *in vivo*. Science 2007;315:107–11.

30. Kurts C, Carbone FR, Barnden M, et al. $CD4^+$ T cell help impairs $CD8^+$ T cell deletion induced by cross-presentation of self-antigens and favors autoimmunity. J Exp Med 1997;186:2057–62.

31. Rosenberg SA, Yang JC, Restifo NP. Cancer immunotherapy: moving beyond current vaccines. Nat Med 2004;10:909–15.

Extralymphatic Tumors Prepare Draining Lymph Nodes to Invasion via a T-Cell Cross-Tolerance Process

Olivier Preynat-Seauve, Emmanuel Contassot, Prisca Schuler, et al.

Cancer Res 2007;67:5009-5016.